Solar Phys (2009) 259: 213–225
DOI 10.1007/s11207-009-9423-9

3D Reconstruction of the Leading Edge of the 20 May 2007 Partial Halo CME

N. Srivastava · B. Inhester · M. Mierla · B. Podlipnik

Received: 22 January 2009 / Accepted: 25 July 2009 / Published online: 2 October 2009

Abstract We have reconstructed the leading edge of a coronal mass ejection (CME) observed on 20 May 2007 by COR1 and COR2 of the SECCHI suite onboard the twin STEREO spacecraft. The reconstruction of the leading edge of this CME was achieved using the tie-pointing method based on epipolar geometry. The true speeds derived from the reconstruction of the leading edge were estimated. These estimated true speeds were compared with the projected plane-of-sky speeds of the leading edge of the CME derived from LASCO aboard SoHO as well as from STEREO A and B images individually. The results show that a better estimation of the true speed of the CME in the Sun – Earth direction is achieved from the 3D reconstruction and therefore has an important bearing on space weather prediction.

Keywords Corona, structures · Coronal mass ejections, initiation and propagation

STEREO Science Results at Solar Minimum
Guest Editors: Eric R. Christian, Michael L. Kaiser, Therese A. Kucera, O.C. St. Cyr

N. Srivastava (✉)
Udaipur Solar Observatory, Physical Research Laboratory, Udaipur, India
e-mail: nandita@prl.res.in

B. Inhester · B. Podlipnik
Max-Planck Institut fuer Sonnensystem Forschung, Katlenburg-Lindau, Germany

B. Inhester
e-mail: binhest@mps.mpg.de

B. Podlipnik
e-mail: podlipnik@mps.mpg.de

M. Mierla
Royal Observatory of Belgium, Brussels, Belgium
e-mail: marilena@oma.be

M. Mierla
Astronomical Institute of the Romanian Academy, Bucharest, Romania

1. Introduction

Coronal mass ejections (CMEs) are responsible for the expulsion of huge quantities of material from the Sun into the interplanetary medium. They are known to play a crucial role in disturbing the space weather environment as they propagate into the interplanetary medium after being expelled from the Sun and interact with the Earth's magnetic field producing strong geomagnetic storms. Generally, fast moving halo CMEs have been known to produce strong geomagnetic storms at the Earth (Gosling *et al.*, 1990; Srivastava and Venkatakrishnan, 2002, 2004). In addition to the speed of the halo CME, the orientation of the magnetic field of the cloud also plays a decisive role, *i.e.*, when the southward component of the interplanetary magnetic field remains so for a long time, a strong geomagnetic storm is probable to occur (Russell, McPherron, and Burton, 1974; Gonzalez and Tsurutani, 1987). Bothmer and Rust (1997), Ruzmaikin, Martin, and Hu (2003), Yurchyshyn, Wang, and Abramenko (2003) also suggested that the magnetic field orientation of the filaments on the solar disk and of the associated magnetic clouds are related. A regular monitoring of solar activity through both a solar disk imager and a coronagraph therefore is essential to forewarn the arrival of a front-sided halo CME. It is also important to accurately measure the line-of-sight velocity of these CMEs, *i.e.*, their speeds in the Sun – Earth direction. However, until now the time-lapse observations of CMEs were limited in the sense that they provided only projected plane-of-sky speeds from the coronagraphic field of view, such as in the case of the Large Angle Spectrometric Coronagraph (LASCO, Brueckner *et al.*, 1995) on SoHO. The measured projected speeds from the time-lapse images of the LASCO coronagraphs were used to estimate the arrival time of the CMEs and resulted in an error of ± 24 hours (see Schwenn *et al.*, 2005 and references therein). Not only halo CMEs, but also, occasionally, limb CMEs may result in strong geomagnetic storms. In fact, many limb CMEs, which had a strong component of velocity in the Sun – Earth direction, were also found to produce strong geomagnetic storms (Schwenn *et al.*, 2005; Gopalswamy *et al.*, 2009). These observations therefore not only call for an accurate estimation of the velocities of CMEs but also of their true direction of propagation right from the time of launch until they reach the outer corona, so that the errors in the estimated time of arrival are kept to minimum. This became possible with the launch of the two identical spacecraft, namely the *Solar TErrestrial RElations Observatory* (STEREO A and B) in October 2006 (Kaiser *et al.*, 2008), which have a set of coronagraphs in the Sun Earth Connection Coronal and Heliospheric Investigation (SECCHI, Howard *et al.*, 2008) package, covering a wide field of view: from 1.4 to 318 $R_{\odot}$. The two STEREO spacecraft orbit the Sun at approximately 1 AU near the ecliptic plane with a slowly increasing angle of separation between them. The rate of increase of the separation angle is approximately 44° per year.

The two views from identical instruments on the two spacecraft allow for stereoscopic observations of the Sun which were not possible earlier. These stereoscopic images are being used to make three dimensional (3D) images of the solar corona in extreme ultraviolet wavelength and white light using the images from the Extreme UltraViolet Imaging (EUVI) instrument and COR1 and COR2 of the SECCHI coronagraphs, respectively (Howard *et al.*, 2008).

2. Reconstruction Technique

Prior to the launch of the STEREO spacecraft, various techniques have been used to infer the 3D structure of features in the solar atmosphere; for example, the techniques developed

by Pizzo and Biesecker (2004) and Inhester (2006). Also, geometric properties of CMEs were studied using a cone model technique (Fisher and Munro, 1984) applied to LASCO data by several authors, *e.g.* Zhao, Plunkett, and Liu (2002), Michalek, Gopalswamy, and Yashiro (2003), Xie, Ofman, and Lawrence (2004), Michalek (2006). The cone model technique is based on the assumption that, above a distance of 2 $R_{\odot}$, CMEs propagate radially with a constant angular width. This implies that the CME shapes remain self-similar through the coronagraphic field of view (Plunkett *et al.*, 1998). Alternatively, Schwenn *et al.* (2005) also found that the ratio between lateral expansion and radial propagation speeds is a constant for most of the CMEs. 3D reconstruction of CMEs was also achieved using the polarization measurements of the white light corona (Moran and Davila, 2004; Dere, Wang, and Howard, 2005). With the launch of the STEREO spacecraft, several techniques are now being evaluated for 3D stereoscopy, using images obtained from two spacecraft. These are mainly based on the tie-pointing (TP) reconstruction; see, *e.g.* Mierla *et al.* (2009) for a comparison of several such reconstruction techniques. In what follows, we briefly describe the salient properties of the different methods used for 3D reconstruction, namely the TP and 3D height – time (3D-HT) methods.

2.1. Epipolar Geometry and Tie-Pointing (TP) Reconstruction Technique

In order to explain the reconstruction technique for STEREO observations, the positions of the two spacecraft can be considered as the two view points of two observers. Any selected point on or above the Sun's surface can be considered as an object to be reconstructed. Together with the positions of the STEREO spacecraft A and B, this point defines a plane called its epipolar plane. Independent of the object chosen, all epipolar planes therefore intersect on the line connecting the two STEREO spacecraft. The special epipolar plane which passes through the Sun center is called the STEREO mission plane (SMP); its normal oriented towards the ecliptic north is the epipolar north direction. From the spacecraft, therefore, all epipolar planes are seen head-on, and project to lines in the spacecraft images, called respective epipolar lines. The fact that any point identified in one image on a specific epipolar line must occur on the same epipolar line in the other image provides a basis for the natural coordinate system that is useful for stereoscopic reconstruction (Inhester, 2006).

The problem of finding the correspondence in the two images obtained by spacecraft A and B, therefore, is reduced to establishing the correspondence only along the equal epipolar lines in both images. On obtaining the association, a 3D reconstruction is possible by calculating the line-of-sight ray that belongs to the respective image positions and back tracing them into the 3D space. As the rays are constrained to lie in the same epipolar plane, they have a well-defined point of intersection. This procedure is called *tie-pointing* (Trucco and Verri, 1998). In particular, the reconstructed points can be presented in different coordinate systems. In this paper, the coordinate system we used is the Heliocentric Earth Equatorial system (HEEQ), which has its z-axis along the solar rotation axis. The x-axis is perpendicular to z and oriented such that Earth lies in the $x-z$ plane (Hapgood, 1992; Thompson, 2006).

2.2. **3D Height – Time (3D-HT) Method**

The height – time technique has been mainly used in the past to determine the plane-of-sky or projected speeds of the CMEs. The measurement or estimation of speeds of the leading edge of CMEs were based on the following steps. (a) Identification of the leading edge at an instant of time. This was possible in white light images taken by LASCO, which measure the

scattered photospheric light by the free electrons in the corona, giving the integrated density along the line-of-sight. (b) Tracking the leading edge in successive time-lapse images in the LASCO field of view. Sheeley *et al.* (1999) developed an automated detection procedure for the faintest moving feature of the CMEs and, using height – time profiles, calculated the projected speeds of these moving features. Recently, Mierla *et al.* (2008) used the 3D-HT technique on the images acquired by COR1 coronagraphs aboard SECCHI/STEREO spacecraft. This technique involves obtaining height – time plots for a well identified feature in a CME from its observations in two STEREO images. This yields two independent projected velocity vectors, from which a 3D velocity vector can be constructed. The height – time profiles were used to determine the true direction of propagation of a CME and also the true propagation speed in the field of view of COR1 *i.e.* up to 4 $R_{\odot}$. Mierla *et al.* (2008) employed this technique for selected features in three CMEs observed by COR1 coronagraphs and found that the method gives a quick and good estimate of both the true direction and speed in the direction of propagation. Thus, this technique serves as a useful and quick tool for space weather forecasting.

3. The Instrument and the Observational Data

For the present study, we used data obtained from COR1 and COR2 coronagraphs of SECCHI on the twin STEREO spacecraft (Howard *et al.*, 2008). The SECCHI is a suite of instruments carrying an Extreme UltraViolet Imager (EUVI) which images the solar disk in four wavelengths, namely, 17.1 nm, 19.5 nm, 28.4 nm and 30.4 nm; two white light coronagraphs, namely, COR1 and COR2 and Heliospheric Imagers (HI1 and HI2) (Howard *et al.*, 2008). The COR1 coronagraph is a classical Lyot-type internally occulted coronagraph that has a field of view from 1.4 to 4 $R_{\odot}$ and observes in white light (Thompson *et al.*, 2003). The COR2 coronagraphs have a field of view from 2.5 to 15 $R_{\odot}$. The COR1 coronagraph has a linear polarizer to suppress the scattered light and obtain polarization brightness from the solar corona. The images are obtained on a CCD with 2048 $\times$ 2048 pixels with a pixel size of 13.5 microns and have a spatial resolution of 7.5 arc-sec. The polarization brightness is obtained from a sequence of three images taken with a polarizer at 0°, 120° and 240°, the cadence of each sequence being either 5 or 10 minutes. The COR2 coronagraph is an externally occulted Lyot coronagraph that observes in white light. Similar to COR1, the COR2 coronagraph also takes a sequence of three linearly polarized images, which are used to obtain the total brightness images. These images are taken with a resolution of 29 arc-sec with a 2048 $\times$ 2048 pixels CCD camera, at a cadence of 30 minutes. We also used white light images taken by LASCO-C2 and -C3 coronagraphs onboard SoHO that have a field of view from 2 to 6 and 3.7 to 32 $R_{\odot}$, respectively (Brueckner *et al.*, 1995). A CME associated with an eruptive filament was observed on 20 May 2007. The associated disk activity was recorded by the EUVI telescope. The CME also displayed the leading edge prominently and therefore was selected as a good candidate for 3D reconstruction. The CME was observed by both COR1 A and B and COR2 A and B. The spacecraft separation angle on 20 May 2007 was 8.63°. We tracked the CME leading edge in COR1 and COR2 images. Figure 1 shows a mosaic of white light CME images observed by COR1 coronagraphs A and B (right and left columns respectively). The three sets were taken at 6:30, 6:50 and 7:10 UT, respectively. A minimum intensity image was obtained for each of the A and B coronagraphs by taking the minimum value for each pixel in all the images of the respective coronagraph for the day the CME was observed. The minimum image of the corona was then subtracted from all the images in order to have a better visualization of the CME leading edge for 3D

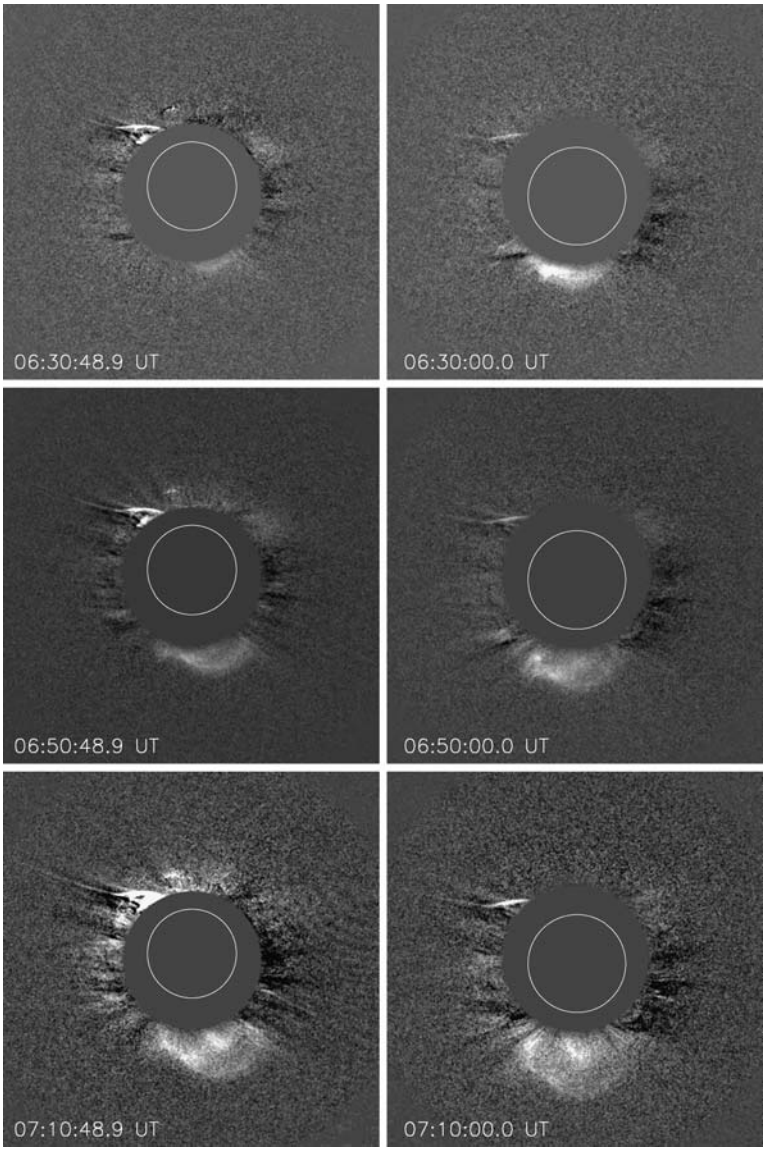

Figure 1 A CME observed on 20 May 2007 by COR1 A (right) and COR1 B (left) coronagraphs. The white circle here represents the solar disk. These images have been rectified such that the images recorded by COR1 B have the same resolution and same solar center as those taken by COR1 A. The images have been rotated such that the epipolar north points up. The upper, middle, and lower panels show the images taken at 6:30, 6:50 and 7:10 UT, respectively.

reconstruction. The CME leading edge was also tracked in the COR2 A and B spacecraft from 8 to 12 UT. The selected images recorded at 8:23, 9:53 and 10:53 UT are shown in Figure 2.

In this paper, we have applied the tie-pointing reconstruction technique to the leading edge of the 20 May 2007 CME recorded by the COR1 and COR2 instruments. We have

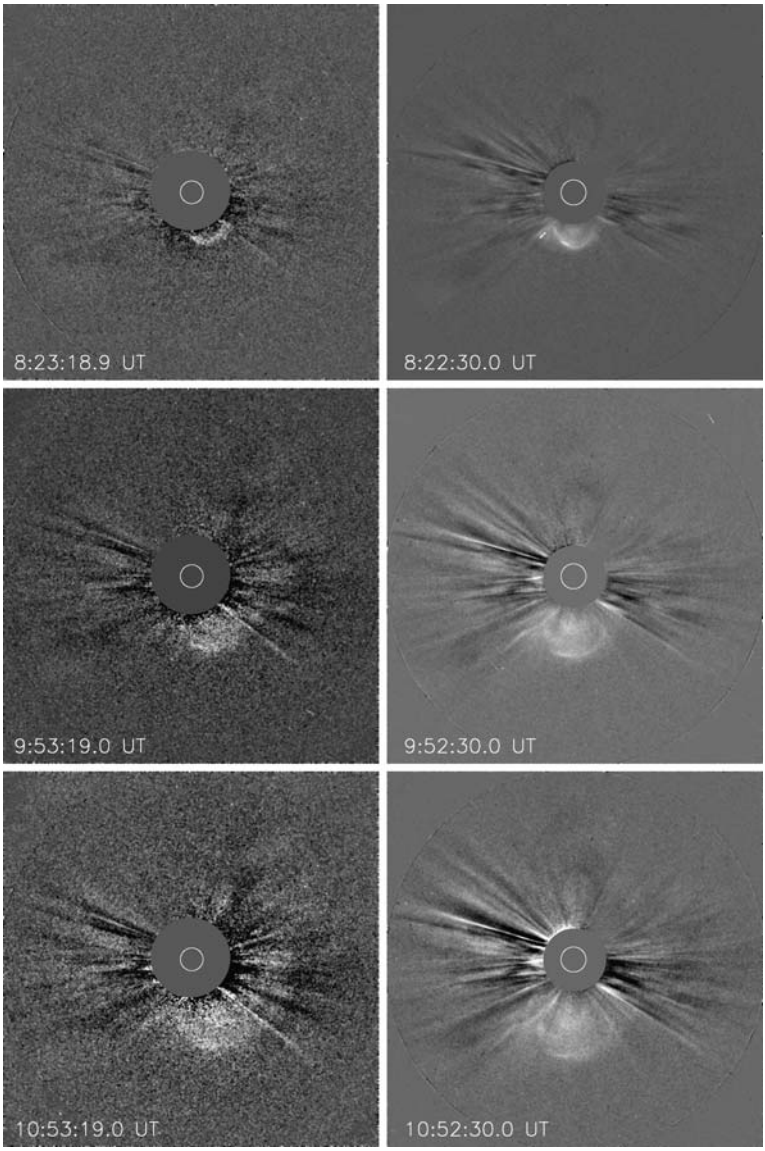

Figure 2 The CME of 20 May 2007 as observed by COR2 A (right) and COR2 B (left) coronagraphs showing its propagation with time. The white circle represents the solar disk. The upper panel, middle and lower panels show the respective images taken at around 8:23, 9:53 and 10:53 UT, respectively. As in Figure 1, the COR2 B images have also been rectified to the same resolution and have the same Sun center as COR2 A images. The images have been rotated such that the epipolar north points up.

compared the true speeds estimated from the reconstructed 3D coordinates using COR1 and COR2 images with those obtained from the height – time technique by Mierla *et al.* (2008) for the COR1 data. We also compare the projected speeds of the leading edge from LASCO-C2 and -C3 images with the estimated true speeds obtained with the TP technique.

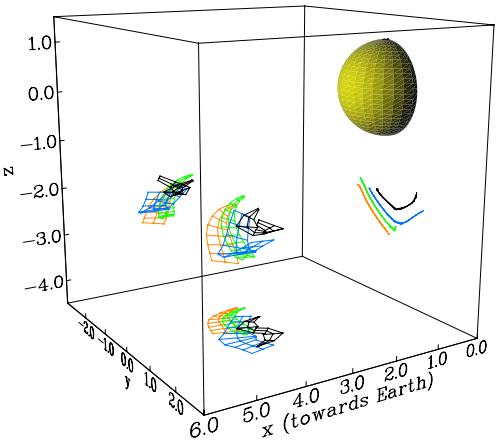

Figure 3 The box shows the reconstructed leading edge of the 20 May 2007 CME, as obtained from the COR1 data. The strips of the CME surface are color coded for different times (*viz.* black for 07:00, blue for 07:10, green for 07:20, and yellow for 07:30 UT). They are shown from an oblique direction and projected on the walls of the box. The coordinate system used is HEEQ.

4. Method for Reconstruction of the CME Leading Edge

We used a tie-pointing method on the stereoscopic images taken by COR1 A and B and COR2 A and B coronagraphs which contain the CME. In order to apply the tie-pointing reconstruction method, the set of images was processed using SECCHI PREP routines. The COR1 coronagraph recorded polarized images taken at three polarization angles, while the images recorded by the COR2 coronagraph included both white light continuum images (no polarizers) and polarized images. By combining polarized images, we derived total brightness images for both COR1 and COR2. For COR2, both sets, *i.e.*, white light continuum images and total brightness images, were used for reconstruction, as they covered different times in CME propagation. Before making the reconstruction, A and B images were rectified such that epipolar north coincides with the y-axis of the images, and the B images were brought to the same resolution and the same Sun center coordinates as the A images. The image headers were then modified accordingly. Further, we used the scc_measure.pro routine available in the SECCHI package of the Solar Software (Freeland and Handy, 1998) to reconstruct the 3D coordinates of several selected points along the leading edge of the CME at an instant. This procedure gives the reconstructed coordinates in terms of heliographic latitude, longitude and distance from the Sun's center. It was applied to the entire image sequence for which the CME was observed in COR1's field of view. The 3D coordinates were also obtained for the leading edge of the CME in the COR2 images by analyzing both white light and total brightness images, the latter summed up from three successive polarization filter observations. This yielded two sets of reconstructed data files for the COR2 data.

5. Reconstruction of the Leading Edge of the 20 May 2007 CME

5.1. 3D Reconstruction of the Leading Edge

The 3D coordinates obtained for various points along the leading edge at various instants of time were plotted for both the COR1 and COR2 data sets and are shown in Figures 3 and 4, respectively. In these plots, different colored lines represent the reconstructed leading edge at different instants. The system of coordinates is HEEQ; its z-axis corresponds to the solar rotation axis and its x-axis points approximately towards the Earth. The plot shows

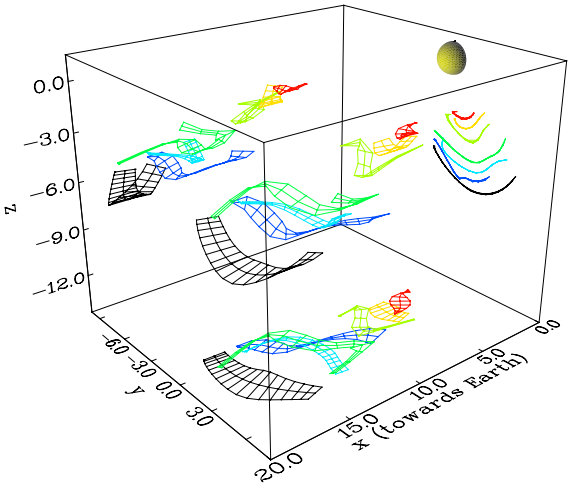

Figure 4 The reconstructed leading edge of 20 May 2007 CME as seen in the COR2 field of view. Here, the strips of the CME surface are color coded for the different times (*viz.* 07:37 for red, 08:10 for yellow, 08:37 for light green, 9:37 for dark green, 10:07 for cyan, 10:37 for blue and 11:07 UT for black), from an oblique direction and also projected onto the walls of the coordinate system. The coordinate system used is HEEQ.

the leading edge from an oblique direction and also projected on the walls of the box. The strips in the plots present the section of the bottom boundary of the CME surface which projects as the leading edge onto the COR1 and COR2 images. We presume that the CME surface is smooth and that the leading edges in the two images correspond to approximately the same outer border on the CME surface. From the fact that both viewing directions are tangential to the reconstructed strip surface, we can derive the local surface normal. The strips in Figures 3 and 4 are thus locally tangential to the CME surface; their widths in the viewing directions correspond approximately to the geometrical reconstruction error if a tie-point localization error of 2 pixels is assumed. Apart from this geometrical error, the errors arising due to the Earth's motion can be considered as negligible. The coordinate system we use is HEEQ, which has its x-axis in the heliographic meridian of Earth. During the 3 hours of observation, the Earth rotates around the Sun by only 0.12°. The errors owing to the Earth's orbital motion are therefore negligible compared to other errors. The reconstructions in Figure 3 are snapshots of this surface section in a 10 minutes time sequence from the COR1 data. In this time, the CME is expected to propagate less than half a solar radius; therefore only a small advance of the surface section in the x- and z-directions can be seen (see the respective projections on the walls, with $z = -4.5$ and $x = 0$). The projection of the background wall with $y = -3$ shows that the propagation in $-z$ is almost as fast as in x. The reconstructions in Figure 4 are similar snapshots of the CME surface as observed from COR2 coronagraphs at different instants from 07:37 to 11:07 UT. During this period, the CME appears to move faster in the x-direction than in the z-direction as can be seen from the respective projections of the CME front on the walls.

It should be noted that we can reconstruct only this small section of the CME surface from the leading edge projections of the CME. The CME itself extends in $+z$-direction from this surface section. The front part of the CME surface which moves towards the Earth is hidden behind the occulter and is, therefore, invisible and not suitable for reconstruction. For space weather predictions, the motion of this front part is, however, most relevant. If a CME evolves self-similarly, as it propagates outwards, there are two speeds which characterize this evolution. One is the speed $V_{\rm cent}$ of the CME center, *e.g.*, the flux rope axis; the other speed $V_{\rm exp}$ refers to the expansion of the intrinsic CME size, *e.g.*, the flux rope diameter. In Figure 5, we show a sketch for the simplified model of a spherically expanding CME front about a propagating center. The figure shows the cross section in approximately the

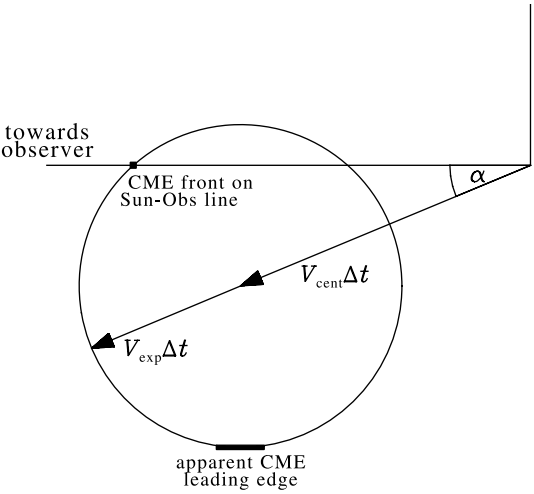

Figure 5 A simple sketch of a CME expanding spherically in a self-similar manner whose center is assumed to propagate radially away from the Sun with V_{cent} and whose radius expands with a velocity V_{exp}. The figure shows a meridional cut through the CME center. Here, α is the propagation latitudinal angle as defined in Section 5.1.

$x-z$ plane with the Sun's center at the origin. The projected CME leading edge and the intersection of the CME front along the Sun – Earth line are marked because their motion can be determined from coronagraphic images and through a travel time estimate from *in-situ* observations, respectively. From straightforward geometry, we obtain the projected speed of the leading edge as $V_{proj} = V_{cent} \sin\alpha + V_{exp}$. Here, α is defined as the propagation latitude angle *i.e.* the angle between the propagation direction and the STEREO mission plane which is very close to the plane of the ecliptic. V_{proj} is always less than the reconstructed 3D speed of the projected leading edge, which is $V_{rec} = \sqrt{V_{cent}^2 + V_{exp}^2 + 2V_{cent}V_{exp}\sin\alpha}$.

The second speed estimate which can be measured only *a-posteriori* is the mean speed from the travel time towards a spacecraft capable of *in-situ* detection of the CME passage. Dividing the spacecraft distance from the Sun by the travel time then yields the mean travel speed, which in our simple model is given by $V_{tt} = V_{cent}\cos\alpha + \sqrt{V_{exp}^2 - V_{cent}^2\sin^2\alpha}$. Another implicit assumption in the comparison of this expression with an empirical mean travel speed is that the CME motion is uniform between the Sun and the observing spacecraft.

The reconstructed speed of the leading edge V_{rec} and V_{tt} are obviously not identical. If there is an empirical proportionality between the propagation and expansion speed, both V_{proj} and V_{tt} become proportional to V_{cent} with different factors of the order of unity. For typical situations where α is small and V_{exp} is not much smaller than V_{cent}, we see that V_{tt} is larger than V_{rec}.

5.2. Height – Time Plot

A particular feature on the leading edge (same feature as traced by Mierla *et al.*, 2008) was identified both in COR1 A and B, and COR2 A and B images, and its projected heights were measured in terms of the solar radius. The same feature was also identified in LASCO-C2 and -C3 images and was tracked with time. The HT plot of the feature is shown in Figure 6. From this plot, it is seen that the feature on the leading edge has an average plane-of-sky speed of 285 km s^{-1} in the field of view of the LASCO, COR1 and COR2 coronagraphs.

The tie-point technique was successfully implemented for several instants of time and the true height and speed of selected points along the leading edge were determined in 3D space. We overplotted the true heights on the plot of projected distances (Figure 6). It is found

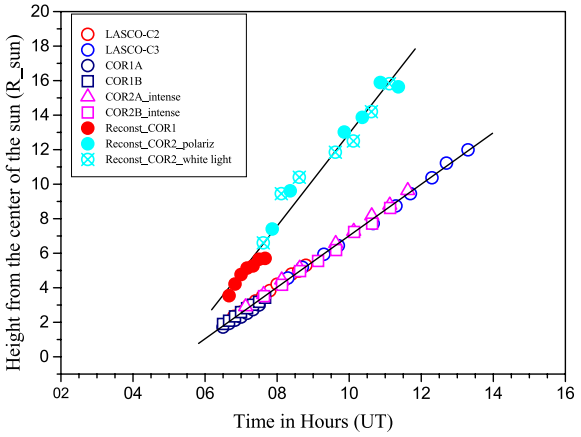

Figure 6 Height – time plot for a selected feature on the leading edge of the CME of 20 May 2007, in the field of view of different coronagraphs. The lower line corresponds to the projection of an identified feature on the leading edge in various coronagraphic fields of view. The upper line represents a linear fit to the reconstructed coordinates plotted as a function of time.

that the projected heights derived from both STEREO spacecraft and from SOHO/LASCO agree to within a few percent, while the reconstructed true heights exceed the projected heights by a factor of 1.80. The same factor applies to the ratio between the true and the projected speeds. For the projected speed, an estimate of 285 km s^{-1} is obtained; the true speed amounts to 510 km s^{-1}. For a solid object ($V_{\rm exp} = 0$ in Figure 5), the inverse of the factor 1.80 should give the sine of the angle between its 3D propagation direction and the spacecraft view direction. In our case, this angle should be $\alpha = 18°$. The assumption of a finite value of $V_{\rm exp}$ requires a smaller propagation angle. For the extreme case, $V_{\rm exp} = V_{\rm proj}$, the angle will vanish altogether. Hence 35° can be considered as the upper bound for α. At the time of the observations, the STEREO A and B were about 8° apart, and their heliocentric angular distances to SOHO were about 4° each. Figures 1 and 2 suggest that the CME propagates closer to the meridional plane of STEREO A than that of STEREO B. From the reconstruction in Figure 4, one may notice that the visible center propagates approximately at a longitude angle of 11° away from the Earth heliographic meridian towards the positive y-axis in the HEEQ system. This should therefore result in a slightly higher projected speed for STEREO B. However, the angles between the different view directions are small and therefore result in approximately the same projected speeds. From the scatter of the reconstructed heights in Figure 6, we estimate the error in the true speed to be about $\pm 10\%$.

We compared the speeds estimated from the reconstruction using the tie-pointing method as obtained in this paper with those obtained by the height – time method by Mierla *et al.* (2008) for the CME of 20 May 2007. The true speeds obtained by Mierla *et al.* (2008) using COR1 data ranging in a field of view from 1.4 to 4 $R_\odot$ were approximately 548 km s^{-1} for an identified feature along the leading edge. The projected speeds for the same feature obtained from images of COR1 A and COR1 B individually were found to be approximately 242 and 253 km s^{-1}. Srivastava (2009) extended the analysis to the COR2 data and estimated an average speed for the field of view between 2.0 to 15 $R_\odot$. They also found that the projected speeds for the same feature obtained from the COR2 A and COR2 B images are approximately 295 and 250 km s^{-1}. Thus the projected speeds measured by Mierla *et al.* (2008) are slightly less than those measured in this paper, while the projected speed measured by Srivastava (2009) for the COR2 A images are similar. The discrepancy in the projected and true speeds obtained using the two methods can be explained as largely due to errors in measurements. However, it may be noted that another factor can also account for this discrepancy. Mierla *et al.* (2008) had used only COR1 data, and their average speed was estimated for

the field of view between 1.4 to 4 $R_{\odot}$, while the projected speeds estimated in this paper are averaged out to 13 $R_{\odot}$. Further, the present study uses projective geometry, while Mierla *et al.* (2008) use affine geometry for the reconstruction. Affine geometry assumes the observer to be at infinite distance, wherein the view directions are practically all parallel, and objects near the Sun appear of the same size independent of the depth h of their position from the plane of the sky, while in the case of projective geometry, the finite distance of the STEREO spacecraft at 200 $R_{\odot}$ is taken into account. The size of the CME appears to be increased by a factor $1 + h/200$ $R_{\odot}$ when it approaches Earth at a distance h from the Sun. With affine geometry, this observed change in size is disregarded and, therefore, projected distances of a CME in front of the Sun are slightly overestimated, depending on h. A comparison of the results of reconstruction of a feature on the leading edge of 20 May 2007 CME using the 3D-HT method and the tie-pointing methods has been made in Srivastava (2009) (*cf.* Table 3). The results show that both reconstruction methods yield similar values for the true speeds of a feature along the leading edge. The small difference arises due to errors in the measurements.

5.3. Travel Time of the CME

A magnetic cloud associated with the CME of 20 May 2007, which was launched at 04:52 UT, arrived at the STEREO A spacecraft on 23 May at 00:56 UT and lasted till 12:24 UT (Kilpua *et al.*, 2008; Liu *et al.*, 2008). The magnetic cloud arrived at STEREO A in approximately 68 hours and its passage was observed for about 11 hours. The measured speed of the magnetic cloud from the *in-situ* measurements was approximately 535 km s^{-1}. Assuming this speed as the average speed of the CME, the estimated travel time is approximately 74 hours. This is in close agreement with the actual travel time of the CME within the measurement errors. The calculations also show that the plane-of-sky speeds do not provide a good estimate of the travel time, which, in the present case, yields 139 hours. A number of recent studies undertaken for the estimation of travel times were based on the plane-of-sky speed of the fastest CME features; see details in Schwenn *et al.* (2005). The authors of this reference also reported that the plane-of-sky speed is not representative of the real radial speed because of projection effects and therefore cannot be used to compute the travel time of the CMEs. Based on the assumption that CMEs propagate and evolve in a self-similar manner and their expansion speeds serve as proxy for the true radial speeds, Schwenn *et al.* (2005) arrived at the following equation: $T_{\rm tt} = 203 - 20.77\ \ln(2V_{\rm exp})$, where $T_{\rm tt}$ is the travel time in hours.

It must be noted, however, that Schwenn *et al.* (2005) defined the expansion speed in terms of the expansion of the CME diameter rather than the radius, and therefore we have substituted $V_{\rm exp}$ in the formula of Schwenn *et al.* (2005) by twice the $V_{\rm exp}$. We calculated the expansion speed using the COR2 A images and found it to be of the order of 146 km s^{-1}. Using this value of expansion speed in the formula above, one obtains a travel time of 85 hours. The difference between the calculated travel time and the actual observed travel time is due to the scatter in the data that were used to derive the formula. By introducing the measured values of expansion speed, projected speed and the reconstructed speed (*i.e.* 146, 285 and 510 km s^{-1}, respectively) in the formulae given in Section 5.1, one can obtain the value of the speed of the CME center $V_{\rm cent} = 445$ km s^{-1}, the value of the propagation angle ($\alpha = 18°$), and $V_{\rm tt} = 467$ km s^{-1}. Substituting the above mentioned values of $V_{\rm cent}$, $V_{\rm proj}$, $V_{\rm exp}$ and α, the mean speed of the CME along the Sun – observer line can be obtained. In the present case, $V_{\rm tt}$ is estimated to be 560 km s^{-1}, which yields a travel time of 73.7 hours. It may also be pointed out here that the travel time calculation is based on the height – time

plot (*cf.* Figure 6) of an identifiable feature along the leading edge, which is irregular in shape. This may not necessarily give the speed and direction of the entire CME. This is in close agreement with the actual travel time, *i.e.*, it is within the measurement errors. These results clearly outline the importance of an estimation of the true speed, which gives better estimates of the travel time.

6. Summary

The tie-pointing reconstruction technique was applied to the 20 May 2007 CME in order to estimate the 3D coordinates of its leading edge. The results show that the tie-pointing and height – time techniques yield similar results for the estimated true speeds of the leading edge, which are approximately 510 $\mathrm{km\,s^{-1}}$ and 548 $\mathrm{km\,s^{-1}}$. In the present case, the true speeds are higher by a factor of 1.8 than the projected speed, which is approximately 285 $\mathrm{km\,s^{-1}}$ as measured individually by each spacecraft. Our results also suggest that both tie-pointing and height – time techniques are effective tools to get true or radial speeds of the leading edge of the coronal mass ejections. The speed of 510 $\mathrm{km\,s^{-1}}$, which is also in agreement with the overall travel time from Sun to Earth, agrees well with the absolute speed we obtained for the CME center from our reconstructions. In this case, it seems that the reduction in speed towards the Earth, which is expected by the deflection of the propagation direction off the Sun – Earth direction by $\sim 18^{\circ}$, is compensated by the intrinsic expansion speed of the CME, *i.e.*, $V_{\mathrm{cent}} \cos\alpha + V_{\mathrm{exp}} \simeq V_{\mathrm{cent}}$. Our study also shows that the CME did not undergo a marked acceleration beyond 10 $R_{\odot}$. If this holds in general, coronagraph observations from the two vantage points as provided by STEREO can provide reliable predictions for the CME travel times. Our study also demonstrates that the reconstructed speeds, which are 1.8 times that of the projected speeds, yield better estimates of the travel time of the CMEs.

This has major implications on the estimation of the arrival time of the CMEs at the Earth. In other words, space weather forecasting can be improved with better and accurate estimates of the initial speeds of the CMEs.

Acknowledgements One of the authors, N.S., would like to acknowledge the Max Planck Institut für Sonnensystemforschung for the financial support for carrying out a major part of this work and also the Royal Observatory of Belgium for financial support for providing local hospitality to finalize the paper. The work at the MPS was supported by DLR contract 50 OC 0501. The authors are grateful to William Thompson and Nathan Rich for their help regarding the software. The authors also would like to thank the STEREO/SECCHI consortium for providing the data. The SECCHI data used here were produced by an international consortium of the Naval Research Laboratory (USA), Lockheed Martin Solar and Astrophysics Lab (USA), NASA Goddard Space Flight Center (USA), Rutherford Appleton Laboratory (UK), University of Birmingham (UK), Max-Planck-Institut for Solar System Research (Germany), Centre Spatiale de Liège (Belgium), Institut d'Optique Theorique et Appliquée (France), Institut d'Astrophysique Spatiale (France).

References

Bothmer, V., Rust, D.M.: 1997, In: Crooker, N., Joselyn, J.A., Feynman, J. (eds.) *Coronal Mass Ejections*, *Geophys. Monogr. Ser.* **99**, AGU, Washington, 139.

Brueckner, G.E., Howard, R.A., Koomen, M.J., Korendyke, C.M., Michels, D.J., Moses, J.D., Socker, D.G., Dere, K.P., Lamy, P.L., Llebaria, A., *et al.*: 1995, *Solar Phys.* **162**, 357.

Dere, K.P., Wang, X., Howard, R.: 2005, *Astrophys. J.* **620**, L119.
Fisher, R.R., Munro, R.H.: 1984, *Astrophys. J.* **280**, 428.
Freeland, S.L., Handy, B.N.: 1998, *Solar Phys.* **182**, 497.
Gonzalez, W.D., Tsurutani, B.T.: 1987, *Planet. Space Sci.* **35**, 1101.
Gopalswamy, N., Yashiro, S., Xie, H., Akiyama, S., Makela, P.: 2009, *Adv. Geosci.*, accepted.
Gosling, J.T., Bame, S.J., McComas, D.J., Phillips, J.L.: 1990, *Geophys. Res. Lett.* **17**, 901.
Hapgood, M.A.: 1992, *Planet. Space Sci.* **40**, 711.
Howard, R.A., Moses, J.D., Vourlidas, A., Newmark, J.S., Socker, D.G., Plunkett, S.P., Korendyke, C.M., Cook, J.W., Hurley, A., Davila, J.B., *et al.*: 2008, *Space Sci. Rev.* **136**, 67.
Inhester, B.: 2006, *Publ. Int. Space Sci. Inst.* astro-ph/0612649, to appear.
Kaiser, M.L., Kucera, T.A., Davila, J.M., St. Cyr, O.C., Guhathakurta, M., Christian, E.: 2008, *Space Sci. Rev.* **136**(1 – 4), 5.
Kilpua, E.K.J., Liewer, P.C., Farrugia, C., Luhmann, J.G., Moest, C., Li, Y., Liu, Y., Lynch, B.J., Russell, C.T., Vourlidas, A., Acuna, M.H., Galvin, A.B., Larson, D., Sauvaud, J.A.: 2008, *Solar Phys.* **254**, 325.
Liu, Y., Luhmann, J.G., Huttunen, K.E.J., Lin, R.P., Bale, S.D., Russell, C.T., Galvin, A.B.: 2008, *Astrophys. J.* **677**, L133.
Michalek, G.: 2006, *Solar Phys.* **237**, 101.
Michalek, G., Gopalswamy, N., Yashiro, S.: 2003, *Astrophys. J.* **584**, 472.
Mierla, M., Davila, J., Thompson, W., Inhester, B., Srivastava, N., Kramar, M., St. Cyr. O.C., Stenborg, G., Howard, R.A.: 2008, *Solar Phys.* **252**, 385.
Mierla, M., Inhester, B., Marque, C., Rodriguez, L., Gissot, S., Zhukov, A., Berghmans, D., Davila, J.: 2009, *Solar Phys.*, in press. doi:10.1007/s11207-009-9416-8.
Moran, T.G., Davila, J.: 2004, *Science* **305**, 66.
Pizzo, V.J., Biesecker, D.A.: 2004, *Geophys. Res. Lett.* **31**, L21802.
Plunkett, S.P., Thompson, B.J., Howard, R.A., Michels, D.J., St. Cyr, O.C., Tappin, S.J., Schwenn, R., Lamy, P.L.: 1998, *Geophys. Res. Lett.* **25**, 14 L2477.
Russell, C.T., McPherron, R.L., Burton, R.K.: 1974, *J. Geophys. Res.* **79**, 1105.
Ruzmaikin, A., Martin, S.F., Hu, Q.: 2003, *J. Geophys. Res.* **108**, 1096.
Schwenn, R., Dal Lago, A., Huttunen, E., Gonzalez, W.D.: 2005, *Ann. Geophys.* **23**, 1033.
Sheeley, N.R. Jr., Walters, J.H., Wang, Y.-M., Howard, R.A.: 1999, *J. Geophys. Res.* **104**, 24739.
Srivastava, N.: 2009, In: Rutten, R., Hasan, S.S. (eds.) *Magnetic Coupling Between the Interior and the Atmosphere of the Sun*, *Astrophys. and Space Sci.*, Springer, Berlin, in press.
Srivastava, N., Venkatakrishnan, P.: 2002, *Geophys. Res. Lett.* **29**(9), 1287.
Srivastava, N., Venkatakrishnan, P.: 2004, *J. Geophys. Res.* **109**(A10), A010103.
Thompson, W.T.: 2006, *Astron. Astrophys.* **449**, 791.
Thompson, W.T., Davila, J.M., Fisher, R.R., Orwig, L.E., Mentzell, J.E., Hetherington, S.E.: 2003, In: Keil, S.L., Avakyan, S.V. (eds.) *Innovative Telescopes and Instrumentation for Solar Astrophysics*, *Proc. SPIE* **4853**.
Trucco, E., Verri, A.: 1998, *Introductory Techniques for 3-D Computer Vision*, Prentice-Hall, Englewood Cliffs.
Xie, H., Ofman, L., Lawrence, G.: 2004, *J. Geophys. Res.* **109**, A03109.
Yurchyshyn, V., Wang, H., Abramenko, V.: 2003, *Adv. Space Res.* **32**, 1965.
Zhao, X.P., Plunkett, S.P., Liu, W.: 2002, *J. Geophys. Res.* **107**, 1223.